CHINESE OPTICS LETTERS

Vol. 19, No. 2 | February 2021

7 kHz sub-nanosecond microchip laser amplified by a grazing incidence double pass slab amplifier

Xu Liu (刘 旭)*, Chaoyong Tan (谭朝勇), Yong Cheng (程 勇), Jingsong Wei (魏靖松), Mengzhen Zhu (朱孟真), Xia Chen (陈 霞), and Chaowei Mi (米朝伟)

Ordnance NCO Academy, Army Engineering University, Wuhan 430075, China

*Corresponding author: 01055108@163.com

Received July 3, 2020 | Accepted September 11, 2020 | Posted Online December 14, 2020

To obtain short pulse width and high peak power laser, a 7 kHz sub-nanosecond microchip laser amplified by a grazing incidence double pass slab amplifier is experimentally demonstrated in this Letter. We use a compact side-pumped Nd:YVO_4 bounce amplifier with grazing incidence beam for achieving high gains and power extraction. Laser output power of 7.37 W at 7 kHz, 1.2 MW pulse peak power with 877 ps duration and 1.05 mJ energy, 25 pm spectral width, and near diffraction limited mode beam quality are achieved, and the optical-to-optical efficiency is 18%. The laser is packaged in a volume of 356 mm × 226 mm × 84 mm and may be used for applications such as laser altimeters and ladar systems.

Keywords: sub-nanosecond; laser amplifier; grazing incidence; bounce laser.

DOI: 10.3788/COL202119.021403

1. Introduction

Many ladar systems and scientific applications such as space-flight laser altimetry for earth science require sub-nanosecond short pulse width and high peak power laser pulses[1–4]. The laser sources should have a narrow linewidth (<50 pm spectral width), high repetition rate [multi-kilohertz (kHz)], short pulse width (<1 ns), high peak power (>1 MW), good beam quality ($M^2 \sim 1.5$), high efficiency, small size, lightweight, and high stability. Compact diode-pumped microchip lasers can achieve sub-nanosecond pulse duration at repetition rates up to several kHz, usually with a passive Q-switch employing Cr^{4+}:YAG saturable absorbers[5,6]. However, the short cavity length of the microchip laser limits the gain volume, the amount of energy that can be stored in the active media is low, and thus microchip lasers with multi-kHz repetition rate and sub-nanosecond pulse duration can reach only very modest output energy, typically up to tens of micro-joules. For some long distance high precision laser ranging and imaging ladar applications, higher energy pulses (>1 mJ) and higher peak power (>1 MW) are usually required[1]. The pathway to higher pulse energies requires the use of higher saturable absorption, which inevitably leads to longer pulse durations and high intracavity power density. A different approach relying on a master oscillator and a high efficiency amplifier stage makes a master oscillator power amplifier (MOPA) configuration become more flexible and power-scalable[7–10].

For the wide absorption and large emission cross sections and proper fluorescence lifetime of Nd:YVO_4 crystals, many diode-pumped Nd:YVO_4 MOPA systems were reported[9–16]. Traditional diode end-pumped Nd:YVO_4 straight amplifiers can be seeded by Nd:YAG lasers or laser diodes (LDs)[9–11]. Side-pumped Nd:YVO_4 bounce amplifiers with grazing incidence beams have been proved to be an excellent design solution for achieving high gains, thus allowing for a significant power extraction with a compact and simple setup[12–16]. Agnesi *et al.* reported a side-pumped Nd:YVO_4 bounce amplifier, 1 MW pulse peak power with 577 ps duration and 545 μJ energy was achieved, and the average output power was 5.45 W at 10 kHz, corresponding to 13% extraction efficiency[14]. Sun *et al.* reported a Nd:YVO_4 grazing incidence slab amplifier with average output power of 20.5 W at 20 kHz and pulse duration of 2.3 ns[17]. Tang *et al.* reported a Nd:YVO_4 slab laser amplifier with grazing incidence and pulse energy of 126 μJ at 100 kHz[18,19]. However, pulse energy up to 1 mJ, sub-nanosecond short pulse width, linearly polarized single longitudinal mode property, and good beam quality lasers are needed for the applications of next-generation, efficient, swath mapping, space-flight laser altimeters.

In this Letter, we demonstrate a 7 kHz sub-nanosecond microchip laser amplified by a grazing incidence double pass Nd:YVO_4 slab amplifier. The configuration can shorten the pulse width and spectral line width by the microchip laser and enhance peak power by the bounce amplifier. The grazing angle of the amplifier has been chosen carefully, where the mode size of the injected seed and the amplifier gain sheet dimensions are well matched. The laser system generates 25 pm spectral line width, 1.05 mJ pulse energy, and 877 ps pulse duration at 7 kHz repetition rate with dimensions of 356 mm × 226 mm × 84 mm. The output power instability reaches ±3%, while the laser has operated continuously for 30 min.

2. Experiments

The schematic diagram for the sub-nanosecond microchip laser and grazing incidence double pass $Nd:YVO_4$ slab amplifier system is shown in Fig. 1. Owing to the good overlap between Nd:YAG and $Nd:YVO_4$ gain bandwidths, we can exploit both materials' favorable characteristics, taking advantage of Nd:YAG physical properties for an efficient passively *Q*-switched oscillator, and design a simple, compact, grazing incidence $Nd:YVO_4$ amplifier configuration.

The master oscillator is a Cr^{4+}:YAG passively *Q*-switched Nd:YAG microchip laser, longitudinally end-pumped by a pulse-driven diode laser, using a pump modulation technique, which can obtain much smaller energy jitter. The microchip is mounted in a thermally controlled holder. By a proper choice of Cr^{4+}:YAG unsaturated transmission and output coupling, the microchip laser is properly set to achieve 3 μJ, 865 ps pulses [Fig. 2(a)] at 7 kHz repetition rate [Fig. 2(b)] (average power 21 mW). The central wavelength is found to locate at 1064.28 nm, and the spectral width is 0.025 nm [Fig. 2(c)]. Diffraction limited mode operation is observed at the repetition rate of 7 kHz. The beam ellipticity is measured to be 0.94, and the beam quality is $M_x^2 = 1.14$ and $M_y^2 = 1.23$ [Fig. 2(d)].

As the fluorescence lifetime of $Nd:YVO_4$ is only about 100 μs, compatible with the injected seed signal, the amplifier's pump diode is set to operate at 7 kHz, and each pump pulse duration is 100 μs. In order to optimize the energy extraction in the $Nd:YVO_4$ slab amplifier, it is also worth noticing that the polarization of the seed and pump beam should be well matched

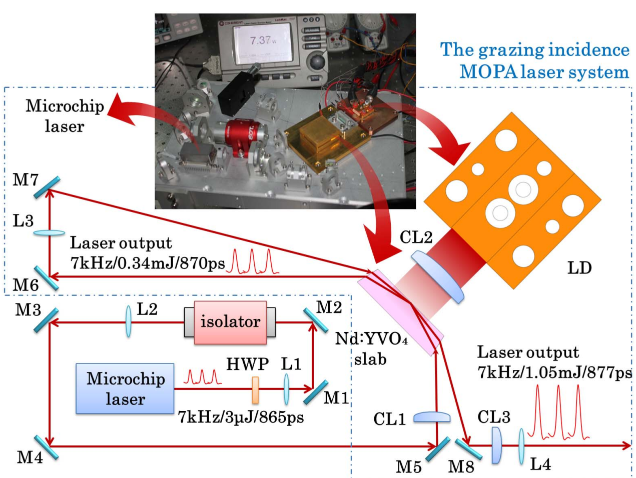

Fig. 1. Setup of the grazing incidence MOPA laser system. $Nd:YVO_4$ slab, *a*-cut slab; HWP, half-wave plate; LD, laser diode, the polarization is parallel to the *c* axis of the $Nd:YVO_4$ slab; M1–M8, high reflectivity mirror; L1–L4, spherical lens, the focal length of L1 is 50 mm, L2 is 75 mm, L3 is 125 mm, and L4 is 75 mm; CL1–CL3, cylindrical lens.

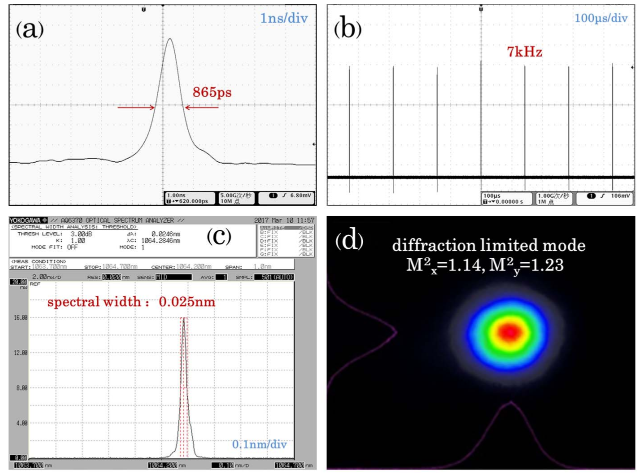

Fig. 2. Output of the master oscillator. (a) The pulse duration, (b) the pulse repetition rate, (c) the output spectrum, and (d) the output beam profile.

for the $Nd:YVO_4$ slab. As the gain property of $Nd:YVO_4$ crystal is polarization relevant, the polarization of the conduction cooled packaged LD is set parallel to the *c* axis of the slab, and a half-wave plate (HWP) is used to control the polarization direction of the seed laser, as shown in Fig. 1.

The *a*-cut $Nd:YVO_4$ crystal is a 22 mm × 5 mm × 1.2 mm, 13° wedged slab. The Nd-doping level is 1% (atomic). The input and output faces of the slab are antireflection (AR) coated at 1064 nm, and the pumped face is AR coated at 808 nm. The two 22 mm × 5 mm faces of the slab are welded to copper heat sink by indium, as shown in Fig. 3(b). The waste heat is transferred by a thermoelectric cooler (TEC). The slab is pumped by a TE polarized CS packaged LD; the maximum pump power is 55 W at 808 nm (25°C). The pump beam is collimated by a cylindrical lens (CL2, shown in Fig. 1), yielding a vertical laser gain sheet of about 200 μm and horizontal gain area of about 10 mm

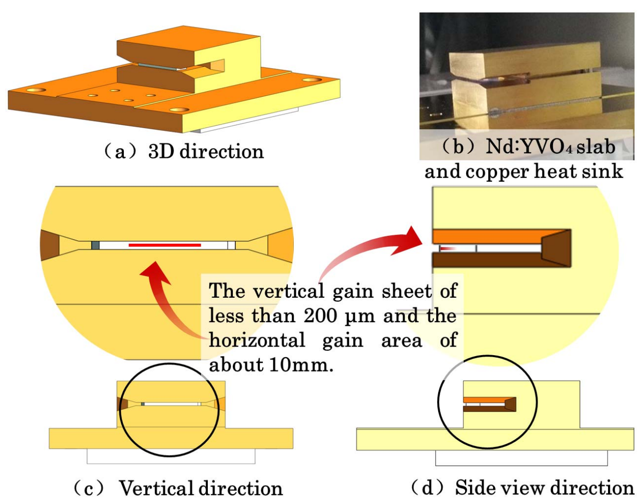

Fig. 3. Schematic diagram of $Nd:YVO_4$ slab and gain sheet. (a) 3D direction, (c) vertical direction, and (d) side view direction of $Nd:YVO_4$ slab and copper heat sink; (b) the actual picture of the module.

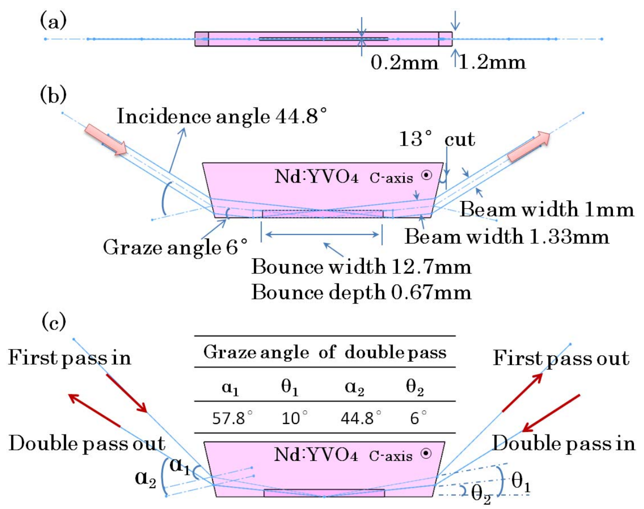

Fig. 4. Design of the grazing incidence of Nd : YVO_4 slab amplifier. (a) The injected beam is reshaped to beam width less than 200 μm by a CL on vertical axis, (b) the grazing angle of 6° can obtain 12.7 mm bounce width and 0.67 mm bounce depth, (c) the grazing angle of double pass.

[shown in Figs. 3(c) and 3(d)]. The polarization of the pump light is parallel to the c axis of the slab. The LD is mounted on a copper heat sink. A TEC is used to control the temperature of the LD. All of the components of the grazing incidence MOPA laser labeled in Fig. 1 are packaged in a volume of 356 mm × 226 mm × 84 mm. The laser engineering prototype is air-cooled. Both the Nd : YVO_4 slab and the LD are set to operate at 25°C.

The optimization of the energy extraction efficiency and the control of the thermal aberrations are achieved by carefully matching the mode size of the injected seed to the amplifier gain sheet dimensions. For that reason, the transverse seed spot needs a different focusing along the vertical and horizontal axes, and the seed beam is reshaped by a CL and then injected into the amplifier. In order to maximize the gain while avoiding clipping effects, the grazing angle has been chosen to be 10° for first pass and 6° for double pass, as shown in Fig. 4(c). For the double pass grazing angle to be 6°, the beam width of 1 mm becomes 1.33 mm on horizontal axis and less than 200 μm on vertical axis inside the amplifier medium, which can obtain a 12.7 mm bounce width and 0.67 mm bounce depth [Fig. 4(b)]. The gain sheet dimensions [Figs. 3(c) and 3(d)] and the pump depth are well matched.

The Faraday magnetic-optic isolator shown in Fig. 1 is necessary for MOPA operation. In the double pass sketch, the backward propagating spontaneous emission originating at the output end of the amplifier may pass through the amplifier twice and be amplified. Then, at the output mirror of the master oscillator, parts of the amplified spontaneous emission (ASE) will reflect back into the amplifier and be quickly amplified along the single pass and double pass beam path because of its extremely high gain; thus, the effective energy extraction efficiency will be decreased. At the same time, the transmitted ASE at the output mirror will feed back into the microchip laser. This effect might increase the number of modes lasing in the microchip and significantly change the master oscillator's spectrum.

The output power curve versus the pump power is shown in Fig. 5. With 41 W diode pump power, a maximum of 2.4 W amplified output power at the pulse repetition rate of 7 kHz is achieved under single pass amplification, and 7.37 W amplified output power is achieved under double pass amplification. The output power extraction efficiency (optical-to-optical efficiency) is 18%; it is a higher extraction efficiency for the sub-nanosecond laser amplifier[14].

Theoretically, the energy of a small-signal light will be increased when passing through the amplifier, and the output fluence can be expressed as[20]

$$E_{\text{out}} = E_s \ln\left\{1 + \left[\exp\left(\frac{E_{\text{in}}}{E_s}\right) - 1\right]\exp(g_0 l)\right\}, \tag{1}$$

where g_0 is the small-signal gain coefficient, l is the length of the gain medium, E_{in} and E_{out} are the energy in the unit area of input and output light, respectively, and E_s is the saturation fluence.

The extraction efficiency η_E is an indicator of the energy release of an amplifier. During the first pass of a small signal, η_E can be written as

$$\eta_E = (E_{\text{out}} - E_{\text{in}})/g_0 l E_s. \tag{2}$$

The gain for the second pass is lower, and the gain coefficient in the expression should be replaced by

$$g_0' = (1 - \eta_E) g_0. \tag{3}$$

With parameters of the slab amplifier used in experiments, a numerical simulation is finished to demonstrate the extreme of amplification. The extraction efficiency curves of single pass and double pass are shown in Fig. 6. The experimental extraction

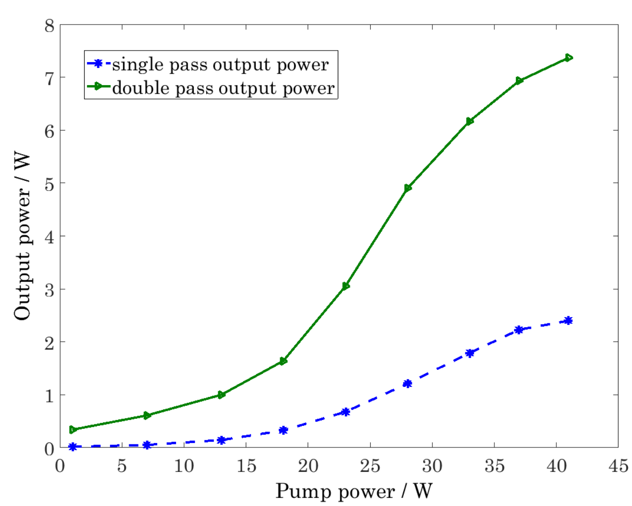

Fig. 5. Output power versus pump power for the single pass and double pass amplification.

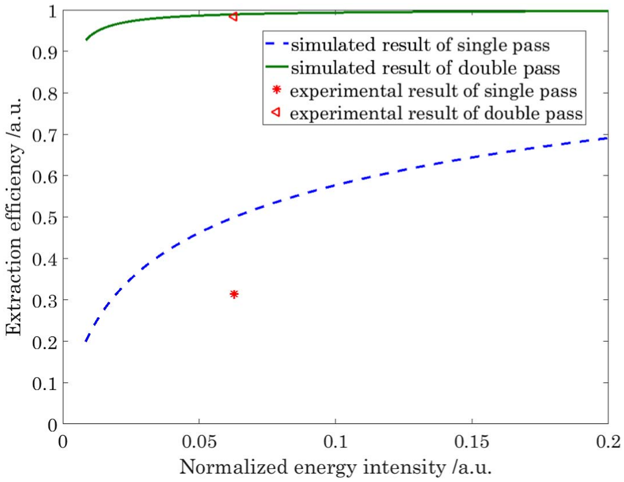

Fig. 6. Extraction efficiency η_E of the gain medium when light passes through it twice; the data of energy intensity on the horizontal axis are normalized to saturation fluence E_s.

efficiency of the two, calculated from the maximal output power in Fig. 5, is pointed out in Fig. 6 as well. Due to the decreasing grazing angle of the double pass, the second one better matches the amplifier gain sheet dimensions and achieves a greater extraction efficiency, which is close to the simulated result.

The spectrum of the double pass amplifier is shown in Fig. 7(a). As the unwanted ASE is suppressed, the spectrum of the double pass amplifier is almost the same as that of the master oscillator, and the spectral width is 0.025 nm too. When increasing the pump power to larger than 41 W, the ASE grows quickly to an unacceptable level. When the pump power increases to 55 W, the ASE power is even larger than the signal power, as shown in Fig. 7(b), and the measured laser emission spectrum consists of two modes spaced 0.22 nm apart. The signal is still located at 1064.28 nm, but the ASE emission is located at 1064.06 nm. For this, the pump power should be limited to not larger than 41 W. The output power instability is measured to be less than ±3%, while the laser has operated continuously for 30 min.

Temporal pulse shapes are observed in Fig. 8. Pulse duration of the double pass laser is about 877 ps [Fig. 8(a)] at 7 kHz [Fig. 8(b)] when the output power is 7.37 W. The amplified pulse

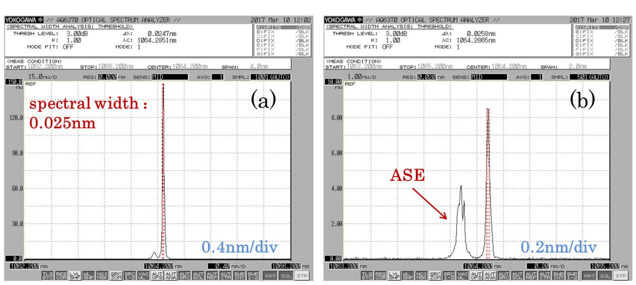

Fig. 7. Output spectrum of the double pass amplification. (a) The output spectrum with 41 W pump power and (b) the output spectrum with 55 W pump power.

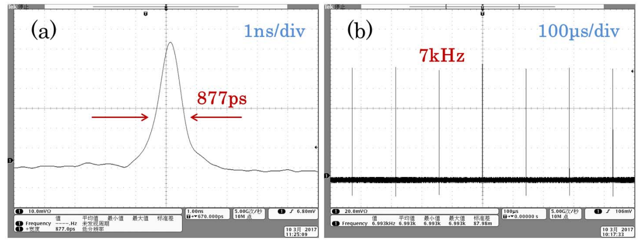

Fig. 8. Waveform of 7.37 W output for the double pass amplifier. (a) The pulse duration and (b) the pulse repetition rate.

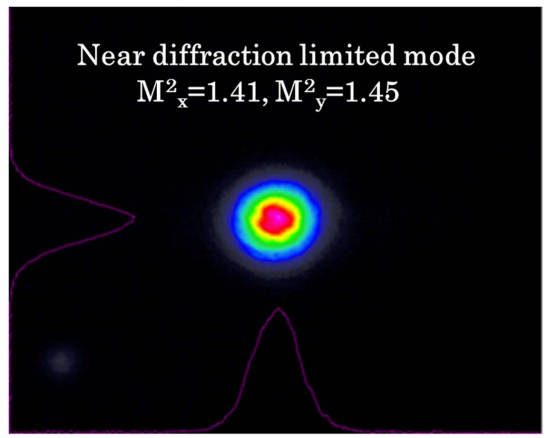

Fig. 9. Output beam profile of the double pass amplifier.

width is found to be nearly the same and becomes slightly wider compared with that of the oscillator. A CL and a spherical lens are used to reshape the amplified beam into a circular symmetrical Gaussian beam. We focus the output beam to a beam waist and measure the diameter of the spot around the waist. The reshaped beam is shown in Fig. 9. The beam ellipticity is measured to be 0.89, less than that of the master oscillator. The double pass beam quality is measured to be $M_x^2 = 1.41$ and $M_y^2 = 1.45$.

3. Conclusions

In conclusion, a 7 kHz sub-nanosecond microchip laser amplified by a grazing incidence double pass $Nd:YVO_4$ slab amplifier is demonstrated. With 41 W diode pump power, laser output power of 7.37 W, 877 ps pulse duration, 25 pm spectral width, and near diffraction limited mode beam quality are achieved. The laser may be used for applications such as laser altimeters and ladar systems.

Acknowledgement

This work was supported by the National Natural Science Foundation of China (NSFC) (No. 61705268), the National

Science and Technology Major Project (No. 2014ZX01005-101-003), and the Innovation Project of Army Engineering University (No. JX2019-01).

References

1. A. W. Yu, M. A. Krainak, D. J. Harding, J. B. Abshire, X. Sun, L. Ramos-Izquierdo, J. Cavanaugh, S. Valett, T. Winkert, M. Plants, C. Kirchner, B. Kamamia, R. Faulkner, P. Dogoda, W. Hasselbrack, and T. Filemyr, "A 16-beam non-scanning swath mapping laser altimeter instrument," Proc. SPIE **8599**, 85990P (2013).
2. Y. Xie, J. Meng, J. Zu, and W. Chen, "Conduction cooling and compact, high peak-power, nanoseconds pluse lasers," Chin. J. Lasers **42**, 0902005 (2015).
3. J. Yun, C. Gao, S. Zhu, C. Sun, H. He, L. Feng, L. Dong, and L. Niu, "High-peak-power, single-mode, nanosecond pulsed, all-fiber laser for high resolution 3D imaging LIDAR system," Chin. Opt. Lett. **10**, 121402 (2012).
4. M. Zhao, C. Wang, Q. Hao, Z. Zou, J. Liu, X. Fan, and L. Su, "High single-pulse energy passively *Q*-switched laser based on Yb,Gd:SrF_2 crystal," Chin. Opt. Lett. **18**, 101401 (2020).
5. C. Yin, L. Huang, M. Gong, P. Yan, Q. Liu, and F. He, "A novel compact side-pumped bonded slab microchip laser," Laser Phys. Lett. **4**, 584 (2007).
6. J. Y. Meng and H. X. Wang, "Single diode-pumped, 1.7 ns microchip laser by Nd:YAG/Cr^{4+}:YAG composite crystal," Laser Phys. **21**, 79 (2011).
7. L. Liu, S. H. Zhou, Y. Liu, and Z. Wang, "The 5.2 kW Nd:YAG slab amplifier chain seeded by Nd:YVO_4 innoslab laser," Chin. Phys. Lett. **34**, 064202 (2017).
8. Y. Zhang, C. Gao, Q. Wang, Q. Na, M. Zhang, M. Gao, and S. Huang, "1 kHz single-frequency, injection-seeded Er:YAG laser with an optical feedback," Chin. Opt. Lett. **17**, 031402 (2019).
9. S. H. Noh, D. J. Kim, and J. W. Kim, "High power generation of adaptive laser beams in a Nd:YVO_4 MOPA system," Chin. Opt. Lett. **15**, 120801 (2017).
10. X. Délen, F. Balembois, and P. Georges, "Direct amplification of a nanosecond laser diode in a high gain diode-pumped Nd:YVO_4 amplifier," Opt. Lett. **39**, 997 (2014).
11. A. Agnesi, P. Dallocchio, F. Pirzio, and G. Reali, "Low-power 100-ps microchip laser amplified by a two-stage Nd:YVO_4 amplifier module," Appl. Phys. B **109**, 659 (2012).
12. J. Morgenweg and K. S. E. Eikema, "Tailored pulse sequences from an 880 nm pumped Nd:YVO_4 bounce amplifier," Opt. Lett. **37**, 208 (2012).
13. K. Nawata, M. Okida, K. Furuki, K. Miyamoto, and T. Omatsu, "Sub-100 W picosecond output from a phase-conjugate Nd:YVO_4 bounce amplifier," Opt. Express **17**, 20816 (2009).
14. A. Agnesi, P. Dallocchio, F. Pirzio, and G. Reali, "Sub-nanosecond single-frequency 10-kHz diode-pumped MOPA laser," Appl. Phys. B **98**, 737 (2010).
15. T. Yoshino, H. Seki, Y. Tokizane, K. Miyamoto, and T. Omatsu, "Efficient high-quality picosecond Nd:YVO_4 bounce laser system," J. Opt. Soc. Am. B **30**, 894 (2013).
16. Z. Sun, Q. Li, Y. Hui, M. Jiang, and H. Lei, "Compact diode-pumped nanosecond Nd:YVO_4 grazing-incidence slab amplifier," Proc. SPIE **9449**, 94491G (2015).
18. C. Tang, S. Xu, X. Zhang, Y. Wang, B. Liu, D. Liu, Z. Xiang, Z. Ye, and C. Liu, "Optimization design of Nd:YVO_4 slab laser amplifier with grazing incidence," Chin. J. Lasers **44**, 1201003 (2017).
19. S. Xu, C. Tang, Y. Wang, F. Zheng, Z. Xiang, D. Liu, X. Zhang, Z. Ye, and C. Liu, "Experimental study of grazing incidence slab laser amplifier with high gain," Chin. J. Lasers **45**, 0101008 (2018).
20. W. Koechner, *Solid-State Laser Engineering* (Springer, 2006).